3.1. INTRODUCTION

The synthesis of palladium nanoparticles (PdNPs) has received closer attention due to its remarkable applications in hydrogenation reactions [Niu *et al*., (2001); Hemantha and Sureshbabu., (2011); Zhang *et al*., (2014)], catalytic oxidation [He *et al*., (2013); Liang *et al*., (2013); Yang *et al*., (2014); Shinde *et al*., (2015)], carbon–carbon bond formation [Narayanan and El-Sayed., (2003); Cheong *et al*., (2010); Shendage *et al*., (2013)], electrochemical reactions in fuel cells [Bianchini and Shen., (2009); Xu *et al*., (2012); Saez *et el*., (2013); Long *et al*., (2013); Ramirez *et al*., (2013)], utilized in hydrogen storage [Rehyani *et al*., (2011); Adams *et al*., (2011); Parambhath *et al*., (2012); Kumar *et al*., (2015); Castillo *et al*., (2015)] and in sensing applications [Mubeen *et al*., (2007); Qin *et al*., (2012); Lu *et al*., (2011); Wang *et al*., (2012); Leng *et al*., (2015); Shin *et al*., (2015);]. Apart from many applications, catalytic activity of PdNPs for probing biochemical interactions has been another area of specific attention. Such applications normally require the dispersion of PdNPs either in homogeneous suspension or in heterogeneous matrix. Accordingly the synthesis of such PdNPs has been a challenging task that enables the synthesis of the PdNPs having dispersibility in desired homogeneous medium and simultaneously may have potentiality for the incorporation within solid state matrix retaining the nanogeometry in order to introduce catalysis during chemical sensor/biosensor designs. During the design of such type of chemical sensors the role of functional alkoxysilane has received greater attention as such precursors enable the formation of nanostructured network which not only act as a matrix for encapsulating small molecule and redox protein but also introduce biocatalysis. Accordingly, the functionalization of PdNPs by functional alkoxysilanes facilitate in tailoring the specific properties of PdNPs for use in a homogeneous or heterogeneous matrix through control over polycrystallinity, morphology and dispersibility. Earlier studies conducted in our laboratory deploy the role of functionalized silane for the formation of thin film of organically modified silicate (ORMOSIL) having nanostructured matrices demonstrating its role in electrochemical biosensors/sensors designs [Pandey *et al*., (2003b); Pandey *et al*., (2001c); Pandey *et al*., (1999c); Pandey *et al*., (1999d); Tripathi, (2002); Sharma (2002); Singh, (2007)]. Such film could be made from the use of functional alkoxysilanes through sol-gel process having most suitable

option for encapsulating the small molecules like ferrocene [Pandey *et al*., (1999e)]. The formation of such nanostructured matrix by controlling the hydrophobic and hydrophilic components of alkoxysilane precursors such as GPTMS, ECETMS, 3-APTMS and TMS has been demonstrated [Pandey *et al*., (1999c); Pandey *et al*., (1999d); Pandey and Upadhyay., (2001b)]. Two combinations of these hydrophobic and hydrophilic alkoxysilanes in appropriate ratio were used for encapsulating the ferrocene monocarboxylic acid (Fc-COOH). The redox electrochemistry of ormosil-encapsulated Fc-COOH in both cases was found to display sluggish reversible electrochemistry mainly due to restricted mobility of ferrocenium ions within nanostructured domain. These findings directed to design ormosil film fulfilling the requirement of ferrocene-mediated bioelectrochemical sensing and the choice of electrocatalyst in combination with encapsulated mediator for facilitating electron transfer process became significant. Fortunately, in our laboratory, the finding on the specific interaction of one of the alkoxysilane precursors like GPTMS and $PdCl_2$ has been recorded [Pandey *et al*., (2001c); Pandey *et al*., (2003b);]. $PdCl_2$ acts as Lewis acid and it reacts with epoxide ring of glycidyl moiety of GPTMS and in turn Pd^{2+}converted into Pd^0 and forming Pd-Glymo complex [Pandey *et al*., (2001c);Sharma (2002)]. The formation of Pd-Si linkage from the interaction of $PdCl_2$ and TMS was also recorded [Pandey *et al*., (2001); Pandey and Upadhyay., (2005a)] that enables the formation of novel nanostructured domains in the presence of palladium-linked GPTMS behaving as a solid solution during bioelectrochemical sensing [Pandey *et al*., (2003a); Pandey *et al*., (2003c);]. The results on the interaction of $PdCl_2$ with GPTMS and TMS revealed following two major conclusions: (1) functionalized alkoxysilane acts as reducing agents for the reduction of metal ions and (2) as generated PdNPs show good affinity with silica matrix [Pandey and Upadhyay., (2005a)]. In addition to reducing ability of GPTMS reports on the use of amino functionalize alkoxysilane [3-(trimethoxysilylpropyl) diethylenetriamine (TMSP diene)] [Zhu *et al*., (2005)] has also been investigated during the synthesis of AuNPs. The time required for AuNPs formation varied from 2 h to 23 h depending on the ratio of TMSP/Au^{3+} [Zhu *et al*., (2005)]. These authors also observed very slow conversion to nanoparticles when 3-APTMS and trimethoxysilylpropyl ethylenediamine were used in place of TMSP.

These findings reveal the reducing and stabilizing ability of 3-APTMS but predict the requirement of additional reducing agent for rapid and controlled nanoparticle synthesis. Accordingly, the investigation on the role of GPTMS alongwith 3-APTMS is sought for the synthesis of PdNPs and has been studied in details in this chapter.

The use of two alkoxysilanes may introduce autohydrolysis, condensation and polycondensation limiting the use of PdNPs made through the active participation of GPTMS and 3-APTMS. Accordingly, it is intended to replace one of the alkoxysilane by suitable organic reducing agent that not only prevent the formation of -Si-O-Si- linkage but precisely control the dispersibility of PdNPs in various solvents of variable polarity. In order to further control the dispersibility of PdNPs in targeted solvents, the use of both hydrophobic and hydrophilic organic reducing agents is attempted during the synthesis of PdNPs. Accordingly, the role of 3-APTMS, Cyclohexanone and THF-HPO has been studied in details during the synthesis of PdNPs with following objectives: (1) Chemical synthesis of PdNPs using 3-APTMS, Cyclohexanone and precursor K_2PdCl_4 under ambient conditions that enables controlled process, solubility, functionality and nanogeometry; (2) Chemical synthesis of PdNPs involving the role of other organic reagent i.e., THF-HPO that enables the synthesis of same in the absence of 3-APTMS; (3) Characterization of the above synthesized nanomaterials using suitable techniques.

3.2. EXPERIMENTAL

3.2.1. Materials

3-aminopropyltrimethoxysilane (3-APTMS), graphite powder (particle size 1-2 μm), Nujol oil (density 0.838 g mL^{-1}), potassium tetrachloropalladate (II) [K_2PdCl_4] and tetrachloroauric acid ($HAuCl_4$) were obtained from Aldrich Chemical Co., India. Tetrahydrofuran (THF) and cyclohexanone were obtained from Merck, India. Tetrahydrofuran hydroperoxide (THF-HPO) was synthesized by autooxidation of THF. All other chemical employed were of analytical grade.

3.2.2. Preparation of Palladium Nanoparticles (PdNPs)

3.2.2.1. Synthesis of PdNPs made through Cyclohexanone and 3-APTMS

PdNPs were synthesized using cyclohexanone in absence and the presence of 3-APTMS. In absence of 3-APTMS 0.005 M methanolic solution of K_2PdCl_4 was mixed with 1.9 M cyclohexanone and allowed to stand at room temperature. And in the presence of 3-APTMS mediated synthesis of PdNPs consisted of following steps: 50mL of 7 mM of K_2PdCl_4 solution in methanol was premixed with 10 mL of methanolic solution of 3-APTMS stirred for 2 min, followed by addition of cyclohexanone. The solution was kept undisturbed for 2 h. PdNPs of black color was obtained within <2 h. The optimum concentrations of cyclohexanone/3-APTMS required for best PdNPs formation was achieved by varying the concentrations of one component while keeping fixed concentrations of another component as shown in Tables 3.1 and 3.2.

Table 3.1. Characteristics of PdNPs as a function of 3-APTMS concentration.

Name	K_2PdCl_4 (M)	3-APTMS (M)	Cyclohexanone(M)	PdNPs formation	Extent of Formation
a	0.005	$0.001x10^{-3}$	1.9	Black	+++
b	0.005	$0.01x10^{-3}$	1.9	Black	++++
c	0.005	$0.1x10^{-3}$	1.9	Black	++++
d	0.005	$1x10^{-3}$	1.9	Light Yellow	-
e	0.005	$3x10^{-3}$	1.9	Light Yellow	-
f	0.005	$5x10^{-3}$	1.9	Light Yellow	-
g	0.005	$10x10^{-3}$	1.9	Light Yellow	-
h	0.005	$50x10^{-3}$	1.9	Light Yellow	-

Table 3.2. Characteristics of PdNPs as a function of Cyclohexanone and 3-APTMS concentration.

S. No.	Cyclohexanone (M)	Extent of formation of PdNPs using 0.005 M K_2PdCl_4 and variable conc. of 3-APTMS (M)		
		$0.001x10^{-3}$	**$0.01x10^{-3}$**	**$0.1x10^{-3}$**
i	0.3	+	+	---
ii	0.6	+	+	---
iii	0.9	+++	++	--
iv	1.4	++++ ($PdNP_1$)	+++	+++ ($PdNP_3$)
v	1.9	++ ($PdNP_2$)	++++	++++ ($PdNP_4$)
vi	2.4	-	-	++
vii	2.8	-	-	-
viii	3.2	-	-	-
ix	3.5	-	-	-
x	3.8	-	-	-

3.2.2.2. THF-HPO and 3-APTMS mediated synthesis of PdNPs

The synthesis of PdNPs involves the mixing of an aqueous solutions of K_2PdCl_4 and 3-APTMS (0.5 M) under stirred conditions over a vertex cyclo mixer followed by the addition of THF-HPO. The mixture turns into light black color within <15 min which subsequently converted to dark black color of PdNPs. Three different compositions were used for the synthesis of PdNPs i.e. $PdNP_5$, $PdNP_6$ and $PdNP_7$ as shown in Table 3.3. All the synthesis was performed at room temperature.

Table 3.3. Compositions of different Palladium nanoparticles (PdNPs) made through 3-APTMS and THF-HPO.

System	K_2PdCl_4 (50 µl) (M)	3-APTMS (10 µl) (M)	THF-HPO (µl)
$PdNP_5$	0.003	1.0	15
$PdNP_6$	0.003	0.5	15
$PdNP_7$	0.003	0.25	15

3.2.3. Measurements and Characterizations

The UV-Vis absorption spectra of samples were recorded in corresponding solvent using a Hitachi U-2900 Spectrophotometer. Atomic force microscope (AFM) image was obtained by a Veeco Nanoscope IV multimode instrument (Veeco Metrology Group, Santa Barbara,CA). Transmission electron microscopy (TEM) studies were performed using Morgagni 268D (Fei Electron Optics) and TEM operating at 200 kV and Philips CM 200 Supertwin TEM. Aqueous solutions were prepared by using doubly distilled-deionized water (Alga water purification system).

3.3. RESULTS

3.3.1. Cyclohexanone and 3-APTMS mediated synthesis of PdNPs

At first instant, it is important to understand the interaction of 3-APTMS and palladium ions if any. It is necessary to understand whether in 3-APTMS, organic amine is playing the central role or alkoxysilane participate in such metal capping. Figure 3.1 A and B and Figure 3.2 A and B show the UV-vis spectra and respective visual images of the interaction between Pd^{2+} ions and 3-APTMS and Pd^{2+} ions with TEOS.

We intended to understand the role of organic moiety that allow the conversion of K_2PdCl_4 into PdNPs. Fortunately, we found that cyclohexanone provide controlled conversion of K_2PdCl_4 into PdNPs in absence of 3-APTMS or as well as in the presence of 3-APTMS was characterized by simple imaging photography. In the presence of 3-APTMS, we examined the formation of PdNPs under two different conditions; (1) keeping constant concentration of cyclohexanone while changing the concentration of 3-APTMS; and (2) keeping 3-APTMS constant while changing the concentrations of cyclohexanone. Figure 3.3 shows the visual photographs of PdNPs made from the use of 0.005 M K_2PdCl_4, 1.9 M Cyclohexanone and variable concentration of 3-APTMS ranging between 0.001×10^{-3} to 50×10^{-3} M as shown in Table 3.1. Under this condition only three concentration of 3-APTMS (0.001×10^{-3},

0.01 x $10^{-3}$and 0.1 x 10^{-3}M) enable the formation of PdNPs (a, b and c) as shown in Figure 3.3. These three concentrations of 3-APTMS were then allowed to investigate the effect of cyclohexanone on the synthesis of PdNPs (Table 3.2 and Figure 3.4-6). Figure 3.7 shows the SAED pattern of the PdNPs in absence of 3-APTMS while similar results in the presence of increasing concentrations of 3-APTMS (0.001 x 10^{-3} and 0.1 x 10^{-3} M) are recorded in Figure 3.8-3.9. Their is the remarkable changes in the morphology of nanomaterials and the plot justifying particle size distribution as shown in Figure 3.10-3.12 of respective PdNPs. The finding shows the average size of PdNPs close to 23.5 nm in the absence of 3-APTMS whereas 15 nm and 7 nm when 3-APTMS is 0.001 x 10^{-3}M, 0.1 x 10^{-3}M respectively.

Figure 3.13-15 shows the dispersibility of as synthesized PdNPs of three concentrations of 3-APTMS (0.001 x 10^{-3}, 0.01 x $10^{-3}$and 0.1 x 10^{-3}M) made using Cyclohexanone in both aqueous and organic solvents viz. water, methanol, acetonitrile and toluene. The data of dispersibility as shown in Table 3.4.

Table 3.4. Dispersibility of PdNPs in water, methanol, acetonitrile and toluene made by using varying concentrations of 3-APTMS and constant concentrations of Cyclohexanone.“+”and“-”sign denotes increasing and decreasing extent of PdNPs dispersibility in the same

S.no.	3-APTMS (M)	Cyclohexanone (M)	Relative dispersibility of PdNPs in various solvents			
			Water	Methanol	Acetonitrile	Toluene
A	0.001x10^{-3}	1.9	++++	++++	++++	----
B	0.01x10^{-3}	1.9	++++	++++	++++	----
C	0.1x10^{-3}	1.9	++++	++++	++++	----

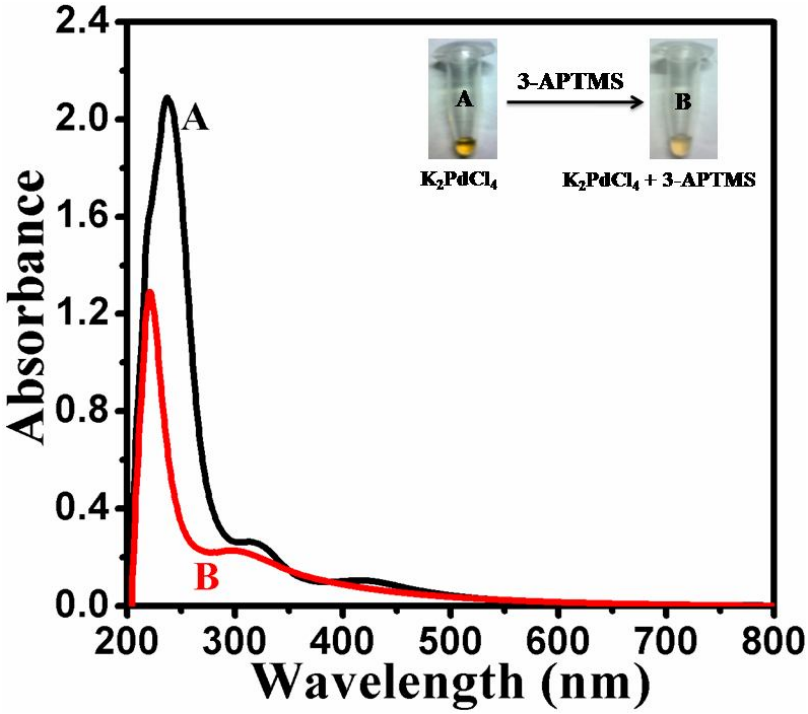

Figure. 3.1. Variation in the UV-vis spectra of methanolic solution ofK_2PdCl_4in absence and the presence of 3-APTMS (A and B) respectively.

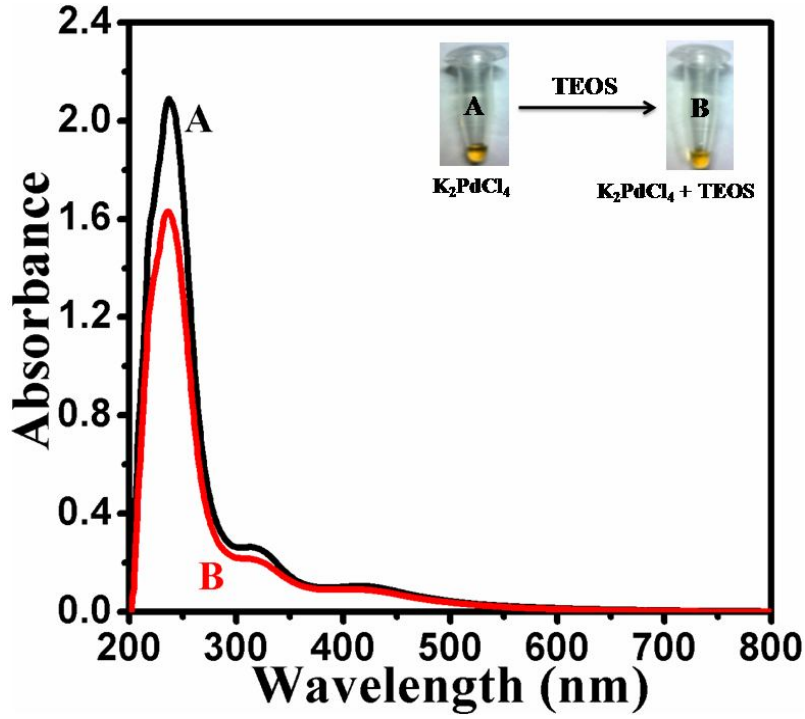

Figure. 3.2. Variation in the UV-vis spectra of methanolic solution ofK_2PdCl_4in absence and the presence of TEOS (A and B) respectively.

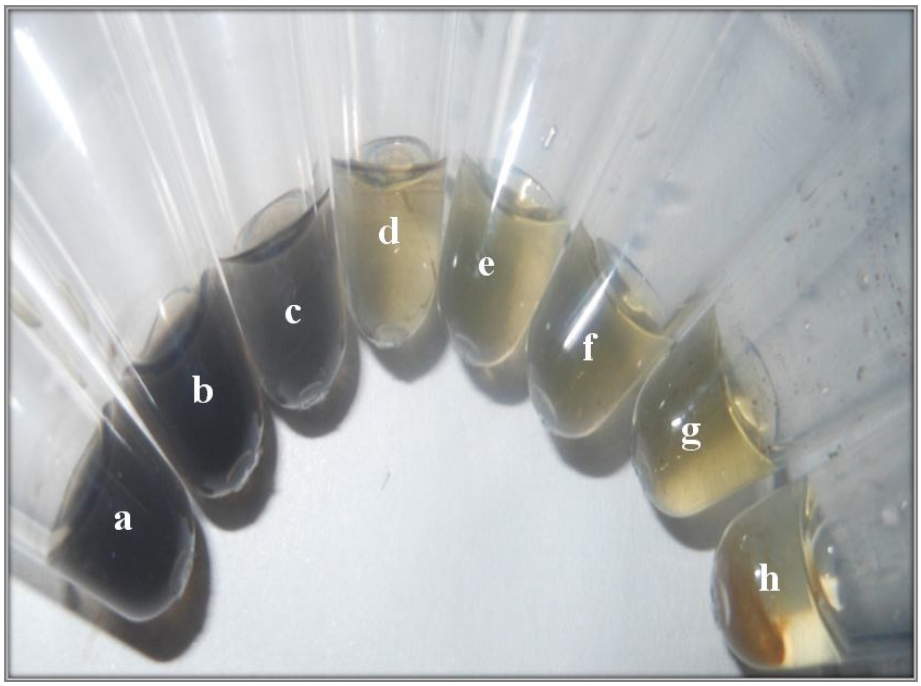

Figure. 3.3. Effect of 3-APTMS concentrations ranging between 0.001 x $10^{-3}$to 50 x 10^{-3}M(images 1–8) on the synthesis of PdNPsfrom 1.9 M cyclohexanone and 0.005 MK_2PdCl_4 as shown in Table 3.2.

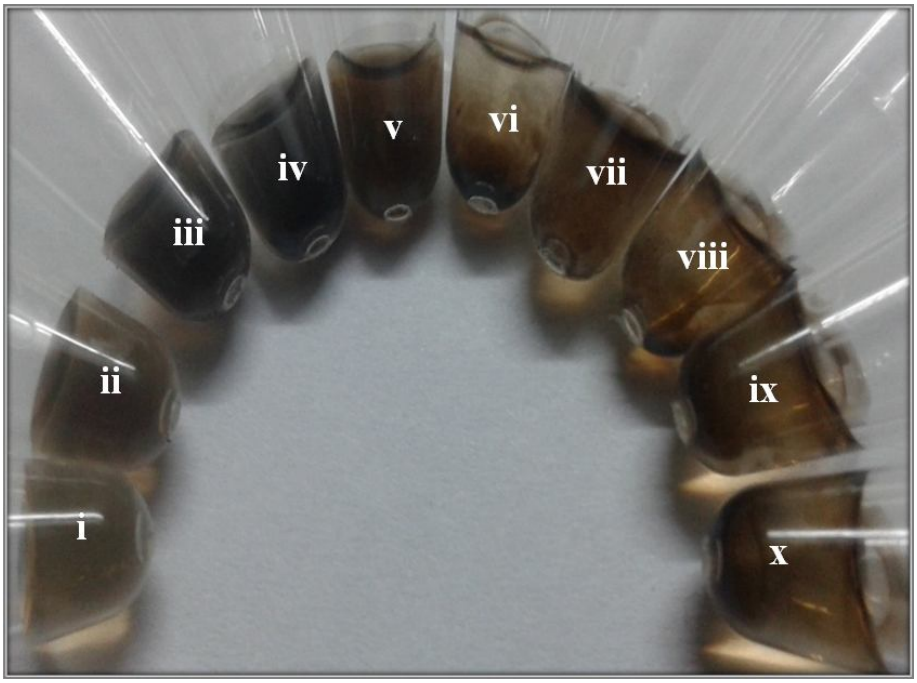

Figure. 3.4. Effect of cyclohexanone concentrations ranging between 0.3 to 3.8M (i–x) on the synthesis of PdNPs from 0.001 x 10^{-3}M3-APTMS and 0.005 M K_2PdCl_4 as shown in Table 3.3.

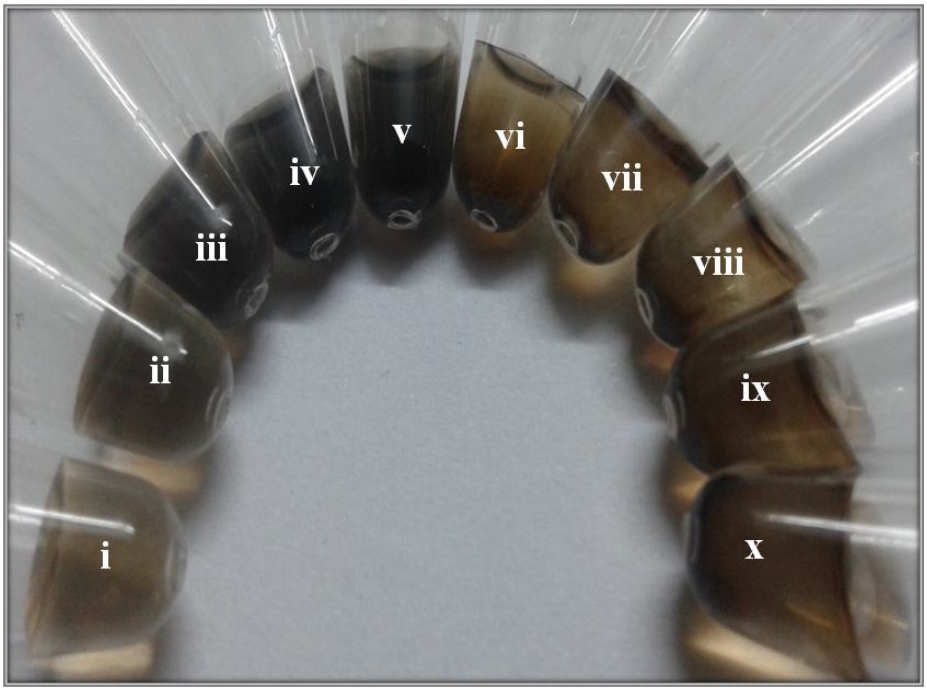

Figure. 3.5. Effect of cyclohexanone concentrations ranging between 0.3 to 3.8 M (i–x) on the synthesis of PdNPs from 0.01 x 10^{-3}M 3-APTMS and 0.005 M K_2PdCl_4 as shown in Table 3.3.

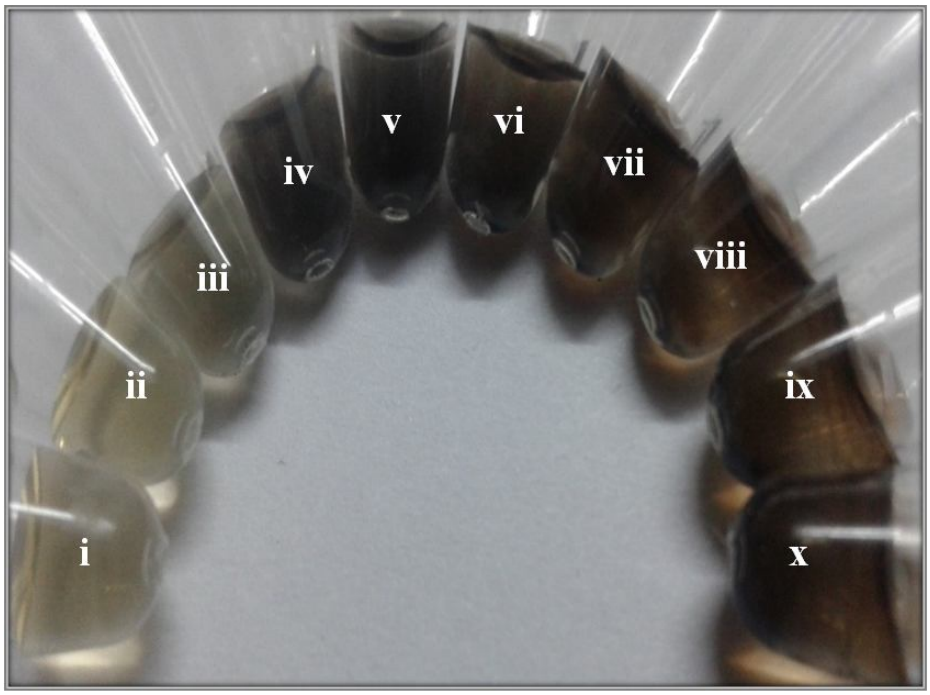

Figure. 3.6. Effect of cyclohexanone concentrations ranging between 0.3 to 3.8 M (i–x) on the synthesis of PdNPs from 0.1 x 10^{-3}M3-APTMS and 0.005 M K_2PdCl_4 as shown in Table 3.3.

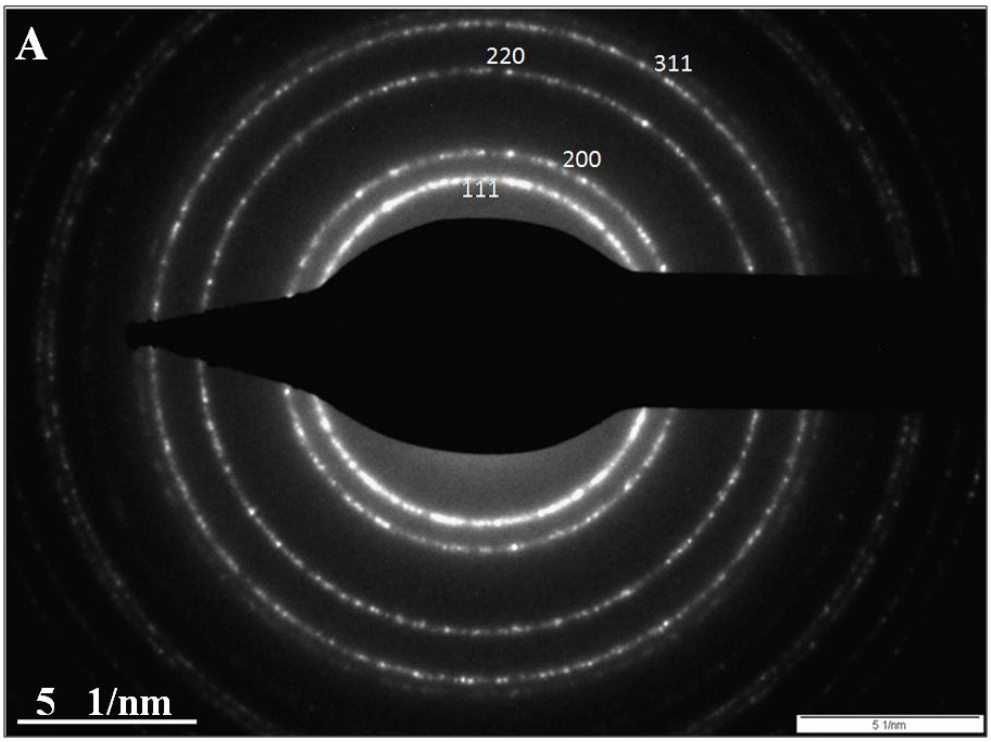

Figure. 3.7. SAED pattern of PdNPs made by using 1.9 M cyclohexanone in absence of 3-APTMS.

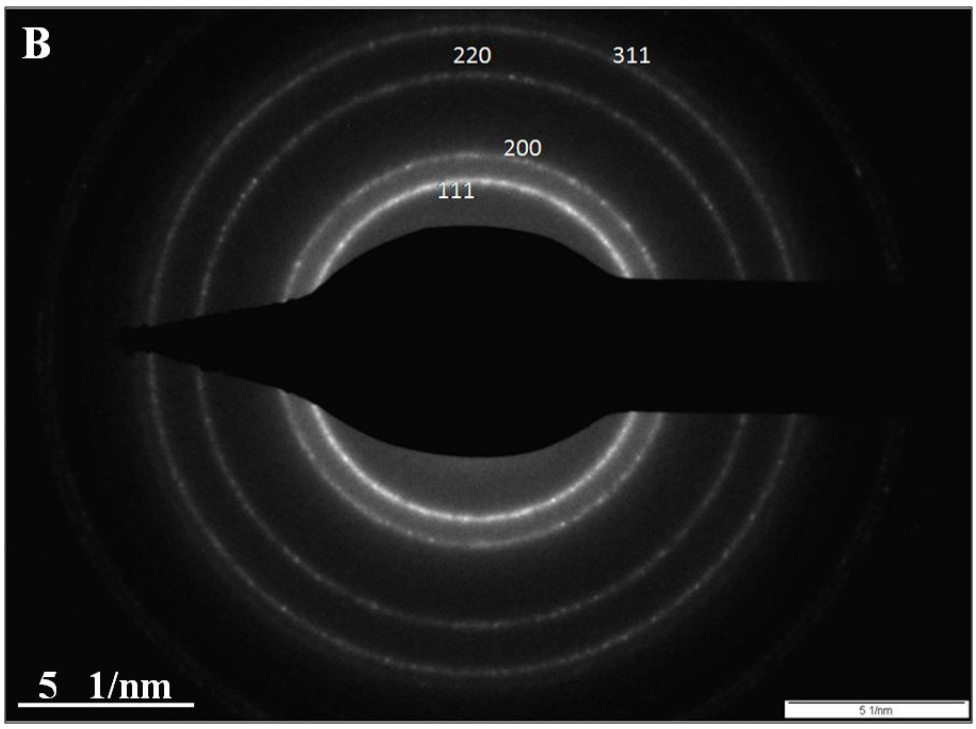

Figure. 3.8. SAED pattern of PdNPs made by using 1.9 M cyclohexanone in presence of 0.001 x 10^{-3}M 3-APTMS.

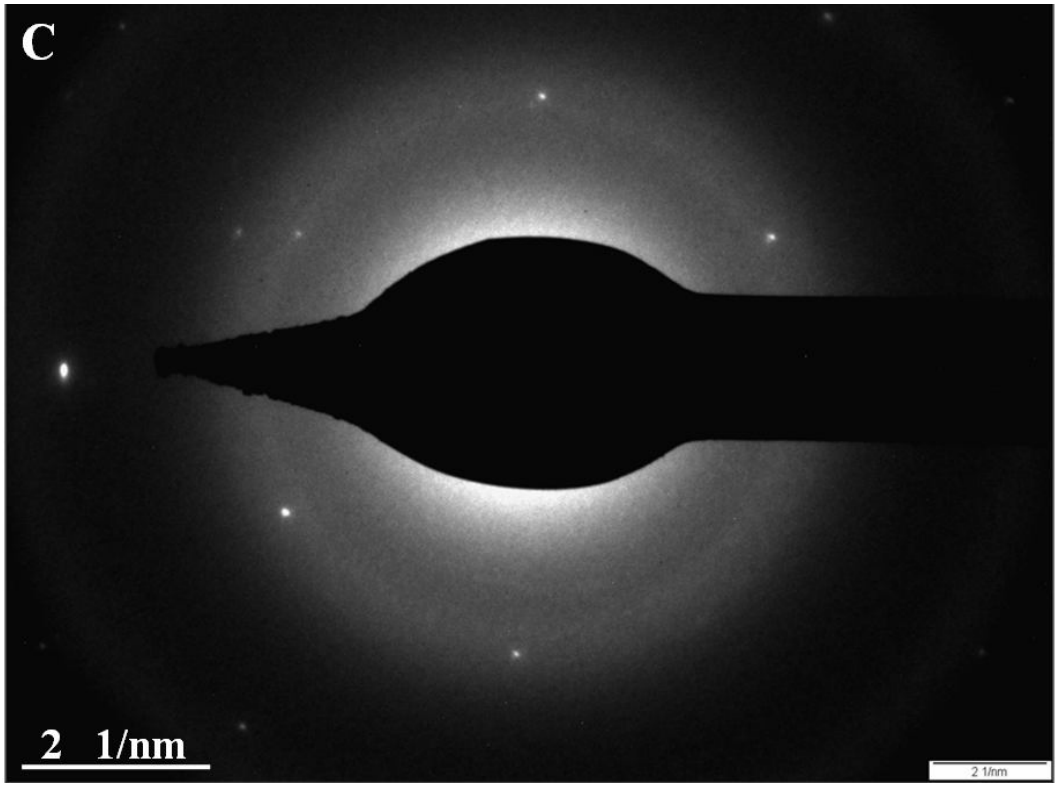

Figure. 3.9. SAED pattern of PdNPs made by using 1.9 M cyclohexanone in presence of 0.1 x 10^{-3}M 3-APTMS.

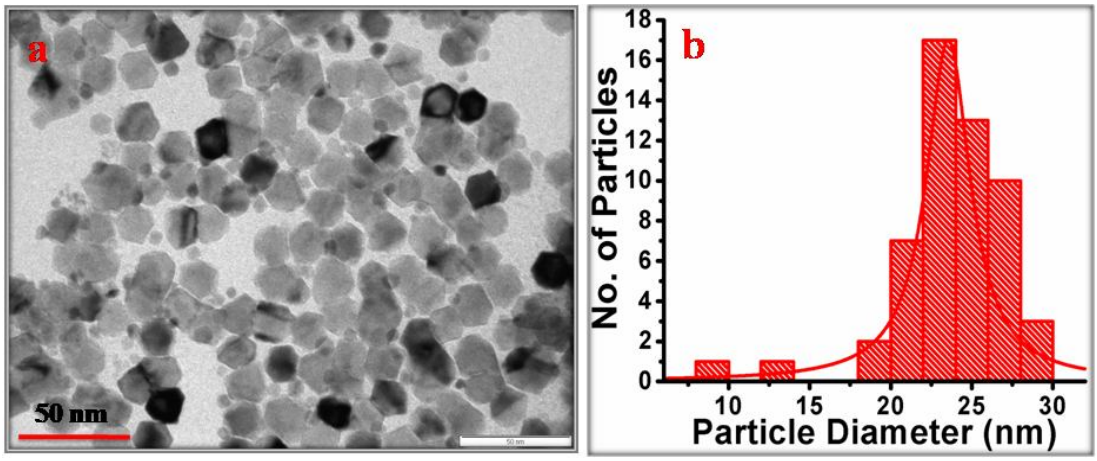

Figure. 3.10. (a) TEM image of PdNPs made by using 1.9 M cyclohexanone in absence of 3-APTMS, **(b)** particle size distribution.

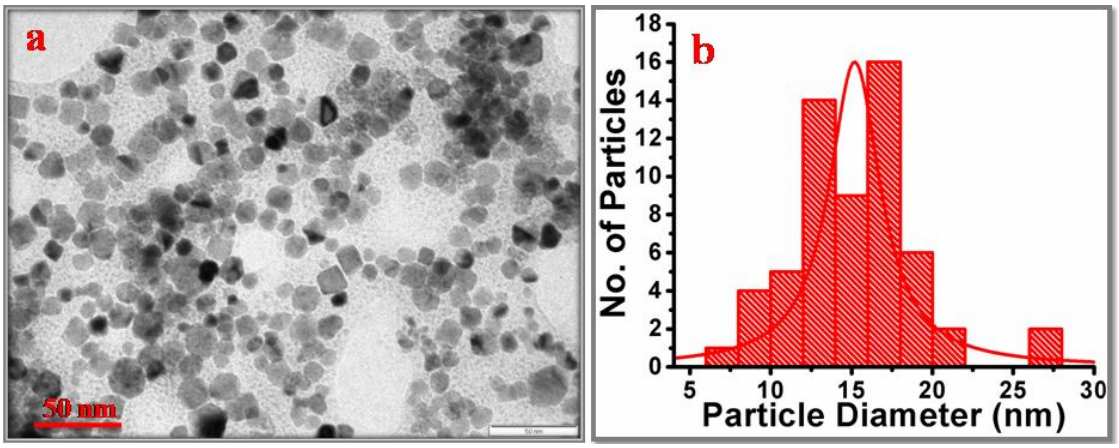

Figure. 3.11. (a) TEM image of PdNPs made by using 1.9 M cyclohexanone in presence of 0.001 x 10^{-3}M 3-APTMS, **(b)** particle size distribution.

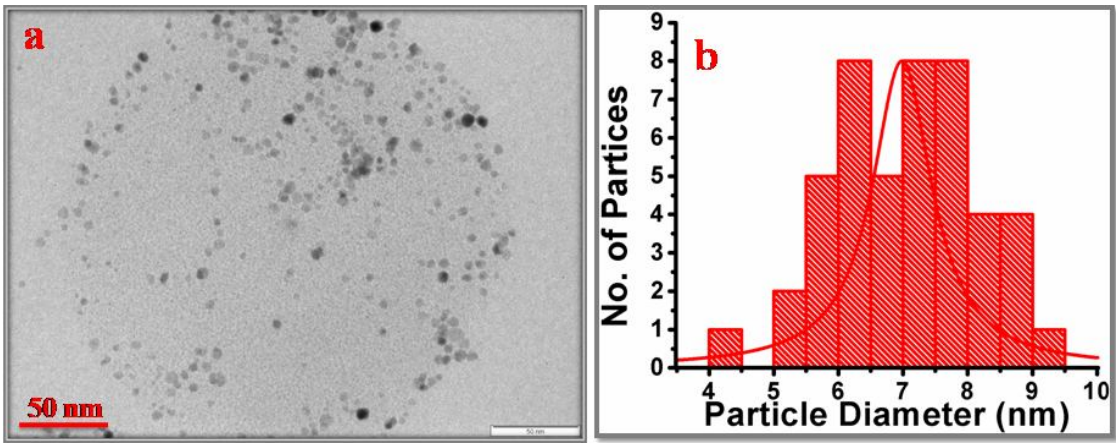

Figure. 3.12. (a) TEM image of PdNPs made by using 1.9 M cyclohexanone in presence of 0.1 x 10^{-3}M 3-APTMS, **(b)** particle size distribution.

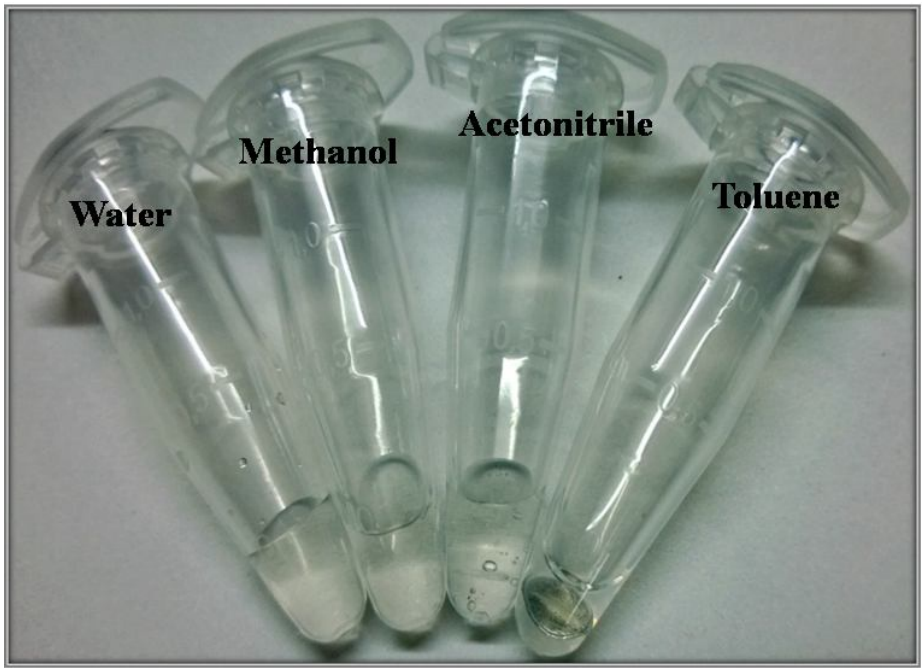

Figure. 3.13. Visual photographs of PdNPs made by using $0.001x10^{-3}$ M 3-APTMS, 1.9 M Cyclohexanone and 0.005 M K_2PdCl_4 as shown in Table 3.5 (A) and their dispersibility in water, methanol, acetonitrile and toluene.

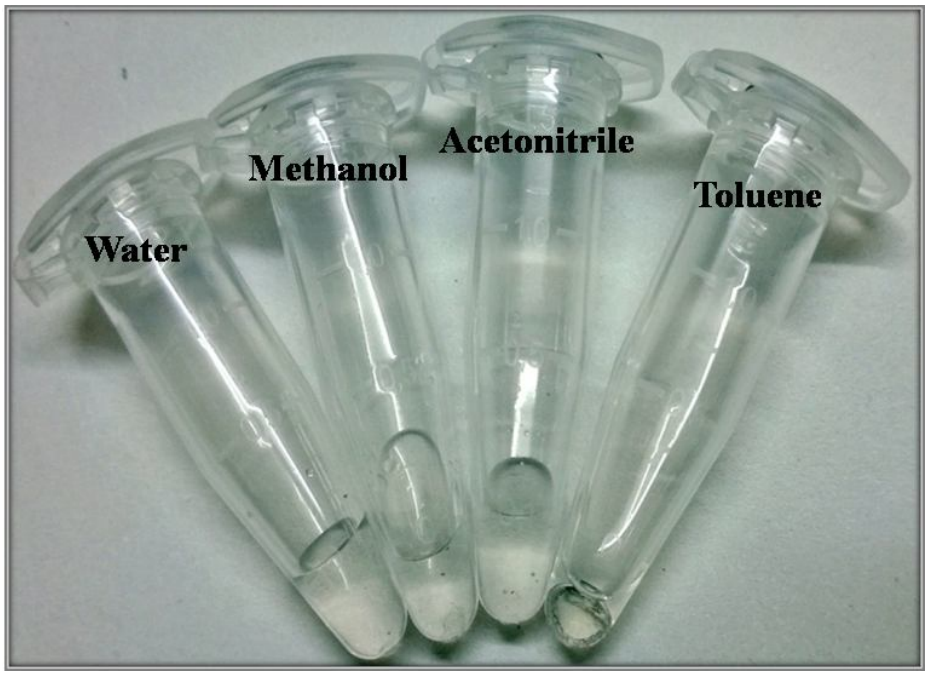

Figure. 3.14. Visual photographs of PdNPs made by using $0.01x10^{-3}$ M 3-APTMS, 1.9 M Cyclohexanone and 0.005 M K_2PdCl_4 as shown in Table 3.5 (B) and their dispersibility in water, methanol, acetonitrile and toluene.

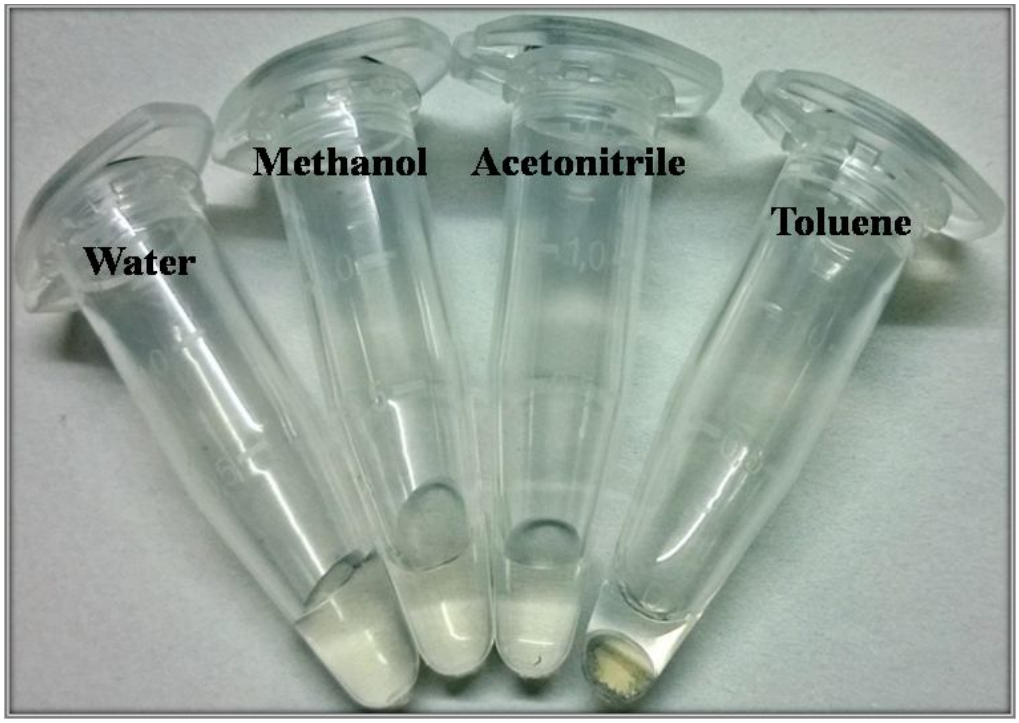

Figure. 3.15. Visual photographs of PdNPs made by using $0.1x10^{-3}$ M 3-APTMS, 1.9 M Cyclohexanone and 0.005 M K_2PdCl_4 as shown in Table 3.5 (A) and their dispersibility in water, methanol, acetonitrile and toluene.

3.3.2. Tetrahydrofuran hydroperoxide and 3-APTMS mediated synthesis of PdNPs

3-APTMS and THF-HPO mediated conversion of K_2PdCl_4 into PdNPs was characterized by UV-Vis spectroscopy and also by simple imaging photography. Figure 3.16 shows the UV-Vis spectra and the photograph of PdNPs (black colour). The as synthesized PdNPs (as shown in Table 3.3) were characterized by TEM. Figure 3.17 and 3.18 depicts the TEM images of the PdNPs. The average particle size was found to be 13.6 and 26.16 nm of $PdNP_1$ and $PdNP_2$. Figure 3.19-3.21 shows the dispersibility of as synthesized PdNPs (as shown in Table 3.3, $PdNP_1$, $PdNP_2$ and $PdNP_3$) made using 3-APTMS and THF-HPO in both aqueous and organic solvents viz. water, methanol, acetonitrile and toluene. The data of dispersibility as shown in Table 3.5.

Table 3.5. Dispersibility of PdNPs in water, methanol, acetonitrile and toluene made by using varying concentrations of 3-APTMS and constant concentrations of THF-HPO. “+”and“”sign denotes increasing and decreasing extent of PdNPs dispersibility in the same

S.no.	3-APTMS (M)	THF-HPO (mg)	Relative dispersibility of PdNPs in various solvents			
			Water	**Methanol**	**Acetonitrile**	**Toluene**
A	0.25	11.4	++++	++++	++++	----
B	0.5	11.4	++++	++++	--	----
C	1	11.4	++++	++++	---	----

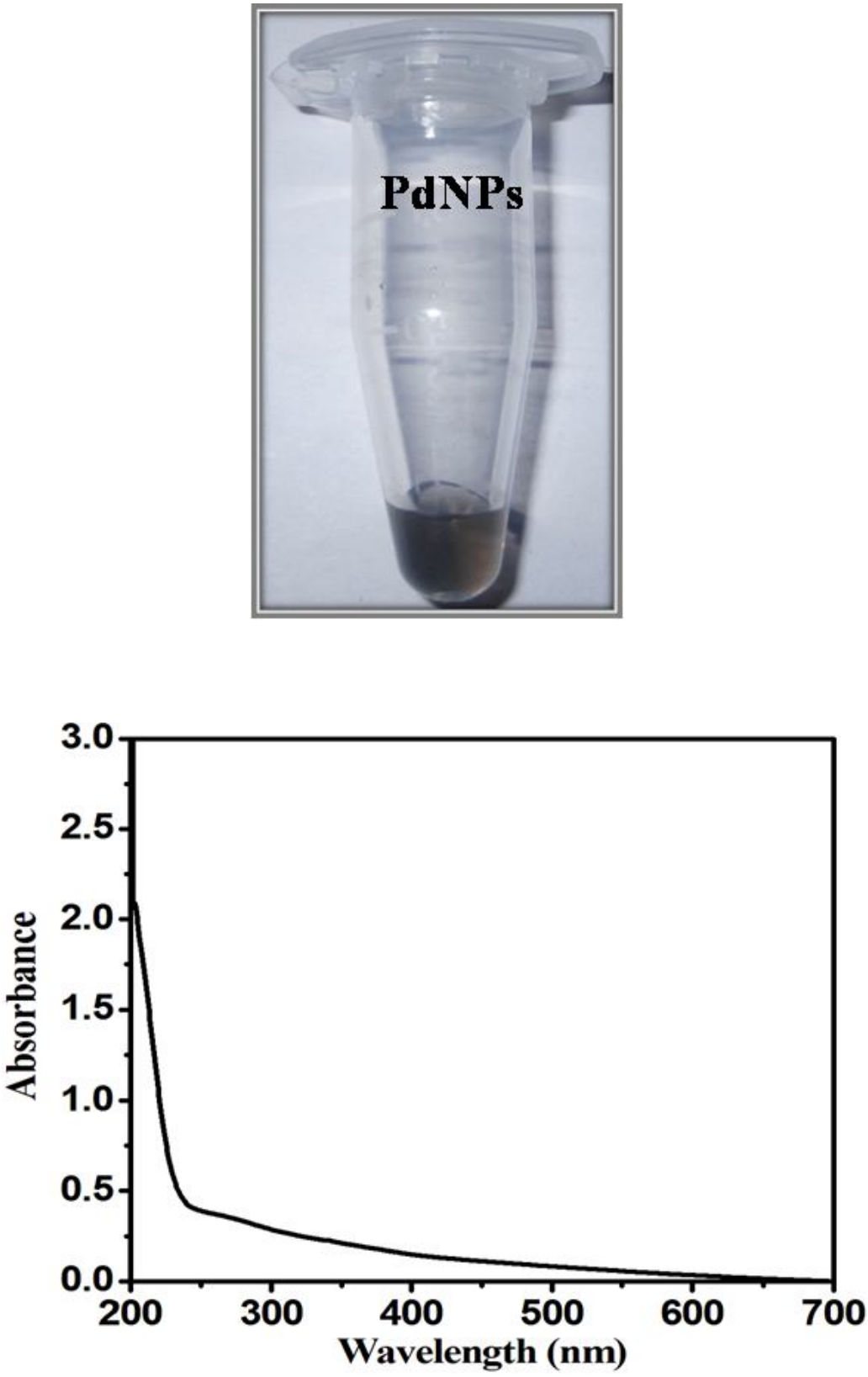

Figure. 3.16. The visual photographs of PdNPs (upper portion). The UV-Vis spectra of the corresponding PdNPs (lower portion).

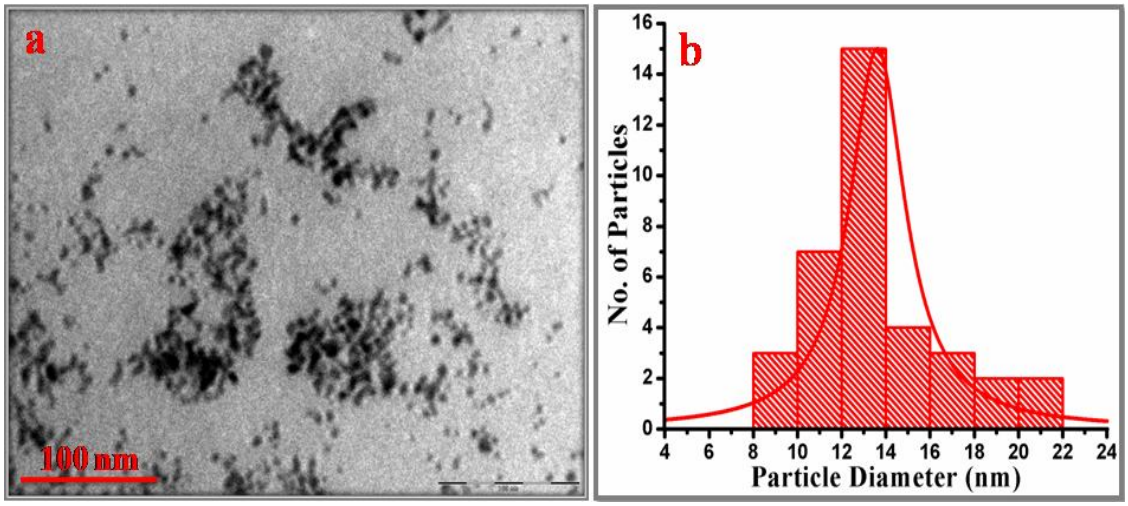

Figure. 3.17. (a) TEM image of PdNPs made by using constant concentration of THF-HPO in presence of 1 M 3-APTMS, **(b)** particle size distribution.

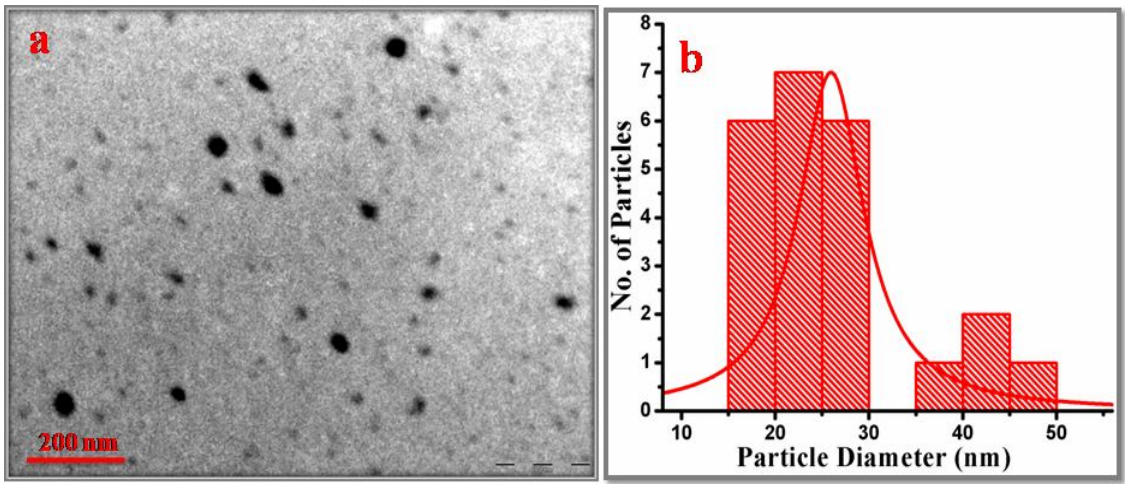

Figure. 3.18. (a) TEM image of PdNPs made by using constant concentration of THF-HPO in presence of 0.5 M 3-APTMS, **(b)** particle size distribution.

Figure. 3.19. Visual photographs of PdNPs made by using 3-APTMS (0.25 M), THF-HPO (11.4 mg) and K_2PdCl_4 (0.003 M) as shown in Table 3.4 and their dispersibility in water, methanol, acetonitrile and toluene.

Figure. 3.20. Visual photographs of PdNPs made by using 3-APTMS (0.5 M), THF-HPO (11.4 mg) and K_2PdCl_4 (0.003 M) as shown in Table 3.4 and their dispersibility in water, methanol, acetonitrile and toluene.

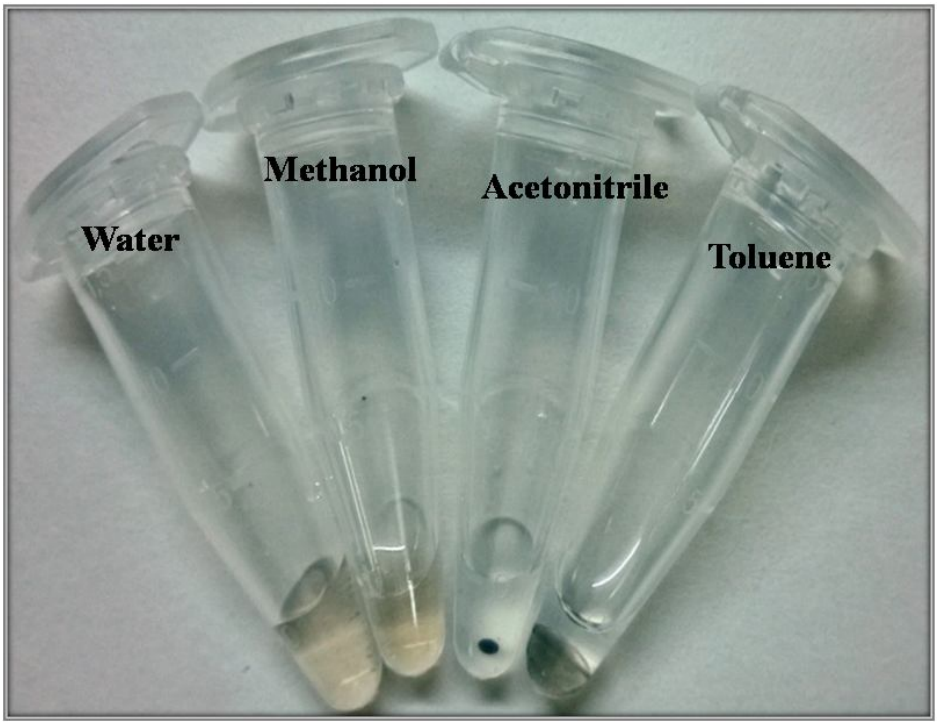

Figure. 3.21. Visual photographs of PdNPs made by using 3-APTMS (1 M), THF-HPO (11.4 mg) and K_2PdCl_4 (0.003 M) as shown in Table 3.4 and their dispersibility in water, methanol, acetonitrile and toluene.

3.4. DISCUSSION

3.4.1. Cyclohexanone and 3-APTMS mediated synthesis of PdNPs

The role of organic amine has been demonstrated during the synthesis of gold and silver nanoparticles. It has been found that Au^{3+}or Ag^{+} undergo specific interaction with 3-APTMS and controlled conversion of 3-APTMS capped metal ions into respective nanoparticles in the presence of suitable organic reducing agent is recorded [Pandey and Chauhan, (2012); Pandey *et al.*, (2014b); Pandey and Pandey, (2014c)]. In order to understand the interaction of 3-APTMS and palladium ions, 3-APTMS has two sites justifying its functional ability for said interaction and to evaluate whether organic amine is playing the central role or alkoxysilane participate in such metal capping, results are shown in Figure 3.1-3.2. The results clearly demonstrate capping of Pd^{2+} by organic amine in Figure 3.1 (A and B) and reveals that the presence of 3-APTMS in K_2PdCl_4 solution decrease in absorption close 420 nm which is characteristic of Pd^{2+} and reflect the possibility for the conversion of oxidation state of the same. It is now important to understand whether 3-APTMS

capped Pd^{2+} are only converted into respective nanoparticles through organic reducing agents or similar organic reducing agent may convert the palladium ions into respective nanoparticles in absence of 3-APTMS as well. Accordingly, Cyclohexanone mediated synthesis of PdNPs has been investigated. Fortunately we found that Cyclohexanone (hydrophobic reducing agent), even being a biphasic system, converts the same into PdNPs. It has been recorded that cyclohexanone converts the Pd^{2+} into PdNPs in the absence of 3-APTMS. The finding reveals that 3-APTMS alone is not able to reduce Pd^{2+} into Pd^{0} whereas Cyclohexanone efficiently convert the same into PdNPs both in absence and the presence of 3-APTMS. In the presence of 3-APTMS, the results based on formation of PdNPs under two different conditions shown in Figure 3.3-6 and data's in Table 3.1-3.2. From Figure 3.3 and Table 3.1 only three concentration of 3-APTMS (0.001×10^{-3}, 0.01×10^{-3} and 0.1×10^{-3} M) enable the formation of PdNPs (a, b and c). These three concentrations of 3-APTMS were then allowed to explore the effect of cyclohexanone on the synthesis of PdNPs. Figure 3.4-6 and Table 3.2 justify the requirement of optimum concentrations of cyclohexanone as a function of 3-APTMS concentrations. Both lower and higher concentration beyond the optimum concentration does not enable the formation of PdNPs (Table 3.2 and Figure3.4-6). Higher concentration of cyclohexanone results into a biphasic system.

The proposed mechanism for the 3-APTMS and cyclohexanone mediated synthesis is shown in Scheme 3.1.

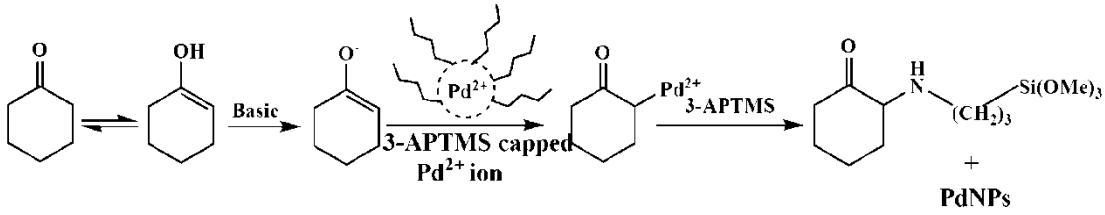

Scheme 3.1. Mechanism of 3-APTMS and Cyclohexanone assisted synthesis of PdNPs.

Cyclohexanone in the prevailing medium undergoes keto-enoltautomerism. Enolate ion acts as an electron donor to 3-APTMS capped Pd^{2+} ion, which in turn acts as a Lewis acid, leading to the formation of PdNPs.

In order to understand, the SAED pattern of PdNPs in absence of 3-APTMS while similar results in the presence of increasing concentrations of 3-APTMS (0.001 x 10^{-3} and 0.1 x 10^{-3} M) are recorded in Figure 3.7-3.9. In absence of 3-APTMS, PdNPs is polycrystalline in nature [Bayliss., (1986); Kim *et al*., (2003); Schlotterbeck *et al*., (2004)]. The electron diffraction pattern, as shown in Figure 3.7, exhibited four sharp rings assigned to (111), (200), (220), and (311) lattice planes with spacing 0.224 nm (111), 0.192 nm (200),0.131 nm (220) of face centered cubic Pd. The results recorded on SAED patterns in the presence of increasing concentration of 3-APTMS (0.001 x 10^{-3} and 0.1 x 10^{-3}) reveal decreases in polycrystallinity of PdNPs as shown in Figure 3.8 and Figure 3.9 respectively. The electron diffraction pattern, as shown in Figure 3.8 for PdNPs made with 0.001 x 10^{-3}M 3-APTMS, exhibited four diffused rings which again tend to diffused at 0.1 x 10^{-3}M 3-APTMS (Figure 3.9) assigned again to Pd lattice. The morphology of PdNPs, evaluated by the TEM as shown in Figure 3.10-3.12(a) and the plot shows the particle size distribution Figure 3.10-3.12(b). There is gradual increase in nanogeometry from Figure 3.10 to 3.12 and justify the role of an organic amine in controlled synthesis of nanoparticles. The results recorded in Figure 3.7 to 3.12 reveals following major observations; (a) decrease in polycrystallinity as a function of 3-APTMS concentrations, (b) an increase in nanogeometry of PdNPs within increase in 3-APTMS concentrations, (c) transition of hexagonal geometry of PdNPs in absence of 3-APTMS into circular morphology in the presence of the same. Such variation in polycrystallinity and microstructure of PdNPs is found mainly due to interaction of silanol residue with as generated PdNPs made in the presence of 3-APTMS enabling an increase in hydrophobic components that restrict the aggregation of as synthesized PdNPs with significant change in morphology on increasing 3-APTMS concentration. While, in case of AuNPs, earlier findings demonstrate [Pandey and Pandey., (2014c); Pandey *et al*., (2014b)] that an increase in 3-APTMS concentration causes decrease in nanogeometry due to hydrophilic behavior of the same allowing the nanoparticles to come closer resulting aggregation of AuNPs with an increase in 3-APTMS concentration.

3.4.2. THF-HPO and 3-APTMS mediated synthesis of PdNPs

As discussed in section 3.4.1 the synthesis of PdNPs made through Cyclohexanone and in the absence or as well as in the presence of 3-APTMS reveals following observations; (1) cyclohexanone allow the formation of PdNPs in absence of 3-APTMS, (2) cyclohexanone also enable the formation of PdNPs in presence of 3-APTMS, (3) the presence of 3-APTMS drastically effect the nanogeometry of PdNPs, and (4) variation in the polycrystallinity and microstructure of PdNPs is found mainly due to interaction of silanol residue in the presence of 3-APTMS. Fortunately, we found that THF-HPO alone is not efficient to convert Pd^{2+} into PdNPs in the absence of 3-APTMS. Accordingly, there is a need to investigate the synthetic protocol for PdNPs that essentially required 3-APTMS. We have demonstrated the reduction of Pd^{2+} by GPTMS has been very well studied in our laboratory in absence of 3-APTMS [Pandey *et al*., (2001c)]. However, 3-APTMS shows excellent affinity for capping Pd^{2+} and that the 3-APTMS capped Pd^{2+} undergo controlled conversion into PdNPs in the presence of GPTMS [Pandey and Chauhan, (2012)]. Due to sensitivity of GPTMS and 3-APTMS towards autohydrolysis, condensation and polycondensation, replacement of GPTMS by other suitable organic reducing agent has been one of our prime attentions. Fortunately, the use of THF-HPO precisely controls the conversion of Au^{3+} into AuNPs [Pandey and Pandey, (2014c)], we intended to understand the conversion of 3-APTMS capped Pd^{2+} into PdNPs. When gold salt was replaced by K_2PdCl_4, it has been found that THF-HPO on mixing with 3-APTMS capped Pd^{2+} ions rapidly converts into a light yellow solution which subsequently leads into black color PdNPs. The observations based on UV-Vis spectroscopy and imaging photography justify the conversion of K_2PdCl_4 into PdNPs. Since the process involves the active participation of 3-APTMS and THF-HPO during the synthesis of PdNPs, it was intended to examine the effect of 3-APTMS concentration on the process of NPs synthesis. Accordingly the formation of PdNPs has examined at three concentrations of 3-APTMS at constant concentration of THF-HPO as shown in Table 3.3. The TEM images of the PdNPs made at 0.5 M and 1 M of 3-APTMS are shown in Figure 3.17-18. The finding reveals an increase in nanogeometry of PdNPs with an increase in the concentration of 3-APTMS similar to that recorded for cyclohexanone and 3-APTMS system discussed in section 3.4.1. The properties of as synthesized PdNPs

justifying novelty of the present process for rapid and controlled synthesis of these nanoparticles under ambient conditions. The time taken during such nanoparticle formation lie between 5 min to 2 h validating the use of 3-APTMS and THF-HPO as most efficient reagents in the synthesis of NMNPs.

The mechanism of nanoparticle synthesis (Scheme 3.2) is found similar as reported earlier [Pandey and Pandey, (2014c)] and may be represented as follows:

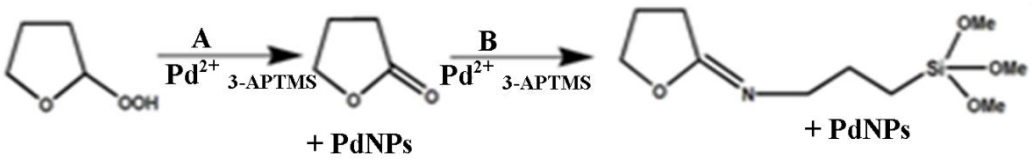

Scheme 3.2. Reaction Mechanism of Tetrahydrofuran hydroperoxide and 3-APTMS mediated formation of PdNPs.

It is again necessary to review the characteristics of reduced $PdCl_2$ by GPTMS and also by THF-HPO in absence and the presence of 3-APTMS. At first instant, the interaction of $PdCl_2$ and GPTMS need to be reviewed as reported earlier [Pandey and Chauhan, (2012)]. GPTMS being completely immiscible in water undergo rapid interaction withaqueous solution of $PdCl_2$. The fast interaction under such condition may be predicted due to two major reasons: (i) $PdCl_2$ acts as Lewis acid and open the epoxide ring of glycidoxy-residue of GPTMS and in turn gets reduced and (ii) reduced palladium has strong affinity to form Pd-C linkage. The possibility for making Pd-C linkage further increases as a function of epoxide ring opening enabling the appearance of active carbon in the system. It is also to be noted that as generated Pd-C tend to become black in appearance and justify the formation of black Pd suspension on immediate mixing of $PdCl_2$ and GPTMS [Pandey *et al*., (2001c)]. On the other hand, when 3-APTMS treated $PdCl_2$ was allowed to interact with GPTMS it does not undergo conversion into black suspension instead slowly turned into light brown color that reflect the recognized color of PdNPs [Pandey and Chauhan, (2012)]. Under this condition, 3-APTMS act as capping agent for $Pd^{2+}$and control the interaction of GPTMS directly with $PdCl_2$ eliminating the

possibility of Pd-C linkage. The color of THF-HPO synthesized PdNPs is also dark black corroborating the formation of active carbon into the medium used for the synthesis of the PdNPs. The formation of butyrolactone may cause the black color of resulting PdNPs (Figure3.16) at first approximation.

3.4.3. Dispersibility of as synthesized PdNPs

Dispersibilityof PdNPs largely depends on the medium which in turn is determined by the apparent polar or nonpolar behavior of the organic reducing agent (Cyclohexanone). The results on the dispersibility of as synthesized PdNPs shown in Figure 3.13-15 are found dispersible in water, methanol and acetonitrile while non-dispersible or insoluble in toluene. And the data as shown in Table 3.4 justify that the PdNPs shows better dispersibility in water, methanol and acetonitrile while not dispersible in toluene.

However, the dispersibility of PdNPs largely depends on the polar or nonpolar behavior of the organic reducing agent (THF-HPO). The results on the dispersibility of as synthesized PdNPs shown in Figure 3.19-3.21. And the data as shown in Table 3.5 justify that the PdNPs shows better dispersibility in water and methanol at all composition that enable the formation of PdNPs. However the dispersibility in acetonitrile is found to be function of 3-APTMS concentration. Higher concentration of 3-APTMS (1.0 M and 0.5 M) restricts dispersibility in acetonitrile whereas PdNPs made at lower concentrations of the same are dispersible in this solvent. The reasons for the variation in dispersibility of PdNPs are due to the micellar behaviour of 3-APTMS and CMC of organic reducing agent.

3.5. CONCLUSIONS

We firstly reported the synthesis of PdNPs using functional alkoxysilane (3-APTMS) and organic reducing agents (Cyclohexanone and THF-HPO). Hydrophobic reducing agent Cyclohexanone for the formation of PdNPs in the absence and presence of 3-APTMS. The synthesis of NPs within 2 h under ambient conditions and the stability is found to be 2 to 3 days. The polycrystallinity and nanogeometry of PdNPs are found as a function of 3-APTMS concentration. Such variation in

polycrystallinity and microstructure of PdNPs is found mainly due to interaction of silanol residue with as generated PdNPs made in the presence of 3-APTMS. The as generated palladium nanoparticles show excellent mimetic ability indicating complete replacement of HRP used in biomedical application.

Hydrophilic reducing agent THF-HPO and 3-APTMS mediated controlled synthesis of PdNPs which allowed the rapid synthesis of the nanoparticles within 5 min to 2 h under ambient conditions are reported and characterized by TEM, and UV-Vis spectroscopy of average size 13.6 and 26.16 nm. The stability of as synthesized PdNPs is found to be 24 to 48 hrs. PdNPs showed better dispersibility in water and methanol while in acetonitrile the dispersibility is the function of 3-APTMS concentration and insoluble in Toluene.